

Fluorogenic Squaraine Dimers with Polarity-Sensitive Folding As Bright Far-Red Probes for Background-Free Bioimaging

Iuliia A. Karpenko,[†] Mayeul Collot,[‡] Ludovic Richert,[‡] Christel Valencia,[§] Pascal Villa,[§] Yves Mély,[‡] Marcel Hibert,[†] Dominique Bonnet,^{*,†} and Andrey S. Klymchenko^{*,‡}

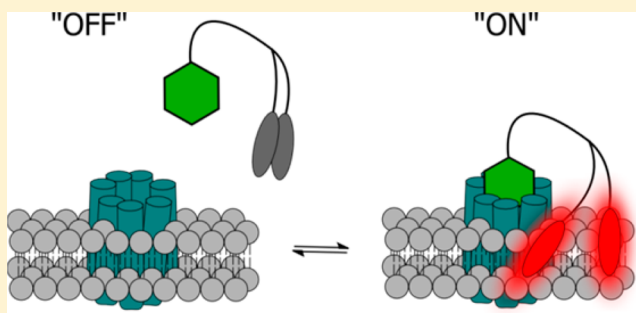
[†]Laboratoire d'Innovation Thérapeutique, UMR 7200 CNRS/Université de Strasbourg, Labex MEDALIS, Faculté de Pharmacie, 74 route du Rhin, 67401 Illkirch, France

[‡]Laboratoire de Biophotonique et Pharmacologie, UMR 7213 CNRS/Université de Strasbourg, Faculté de Pharmacie, 74 route du Rhin, 67401 Illkirch, France

[§]Platform of Integrative Chemical Biology of Strasbourg (PCBIS), FMTS, UMS 3286 CNRS/Université de Strasbourg, ESBS Pôle API, Bld Sébastien Brant, 67401 Illkirch, France

S Supporting Information

ABSTRACT: Polarity-sensitive fluorogenic dyes raised considerable attention because they can turn on their fluorescence after binding to biological targets, allowing background-free imaging. However, their brightness is limited, and they do not operate in the far-red region. Here, we present a new concept of fluorogenic dye based on a squaraine dimer that unfolds on changing environment from aqueous to organic and thus turns on its fluorescence. In aqueous media, all three newly synthesized dimers displayed a short wavelength band characteristic of an H-aggregate that was practically non-fluorescent, whereas in organic media, they displayed a strong fluorescence similar to that of the squaraine monomer. For the best dimer, which contained a pegylated squaraine core, we obtained a very high turn-on response (organic vs aqueous) up to 82-fold. Time-resolved studies confirmed the presence of nonfluorescent intramolecular H-aggregates that increased with the water content. To apply these fluorogenic dimers for targeted imaging, we grafted them to carbetocin, a ligand of the oxytocin G protein-coupled receptor. A strong receptor-specific signal was observed for all three conjugates at nanomolar concentrations. The probe derived from the core-pegylated squaraine showed the highest specificity to the target receptor together with minimal nonspecific binding to serum and lipid membranes. The obtained dimers can be considered as the brightest polarity-sensitive fluorogenic molecules reported to date, having $\sim 660,000 \text{ M}^{-1} \text{ cm}^{-1}$ extinction coefficient and up to 40% quantum yield, whereas far-red operation region enables both *in vitro* and *in vivo* applications. The proposed concept can be extended to other dye families and other membrane receptors, opening the route to new ultrabright fluorogenic dyes.



■ INTRODUCTION

Fluorogenic and chromogenic probes, which turn on their fluorescence in response to a target, have attracted considerable attention as new tools for molecular sensing in biology.¹ As they are nonfluorescent in their free form, they can drastically decrease the background and thus improve the signal-to-background ratio in fluorescence detection and imaging. Particularly interesting are the environment-sensitive probes, which decode variation in their molecular surrounding into fluorescence turn-on or change in their emission color. Fluorogenic and chromogenic responses are usually achieved by mechanisms such as charge and electron transfer in case of polarity-sensitive (solvatochromic) dyes,² internal conversion due to molecular rotation (molecular rotors),³ or proton transfer.⁴ Their capacity to provide fluorescence turn-on or color change in response to changes in their molecular environment, polarity in particular, resulted in a variety of

applications^{1c,5} including monitoring interactions of peptides with proteins,⁶ nucleic acids,⁷ and lipids⁸ as well as ligand-receptor binding⁹ and protein conformational changes.¹⁰

However, these probes show several crucial drawbacks. First, most of them are excited in the blue region, and there are practically no examples of polarity-sensitive fluorogenic dyes operating in far-red region (630–700 nm), which is a perfect window for biological applications *in vitro* and *in vivo*. Second, these probes display limited brightness due to the small extinction coefficients of their push-pull chromophores ($< 60,000 \text{ M}^{-1} \text{ cm}^{-1}$) compared to cyanine or merocyanine dyes.^{5a} This is a crucial limitation for the development of high-sensitivity biomolecular assays. Finally, polarity-sensitive dyes with red-shifted absorption (e.g., Nile Red)¹¹ present much

Received: October 29, 2014

Published: December 15, 2014

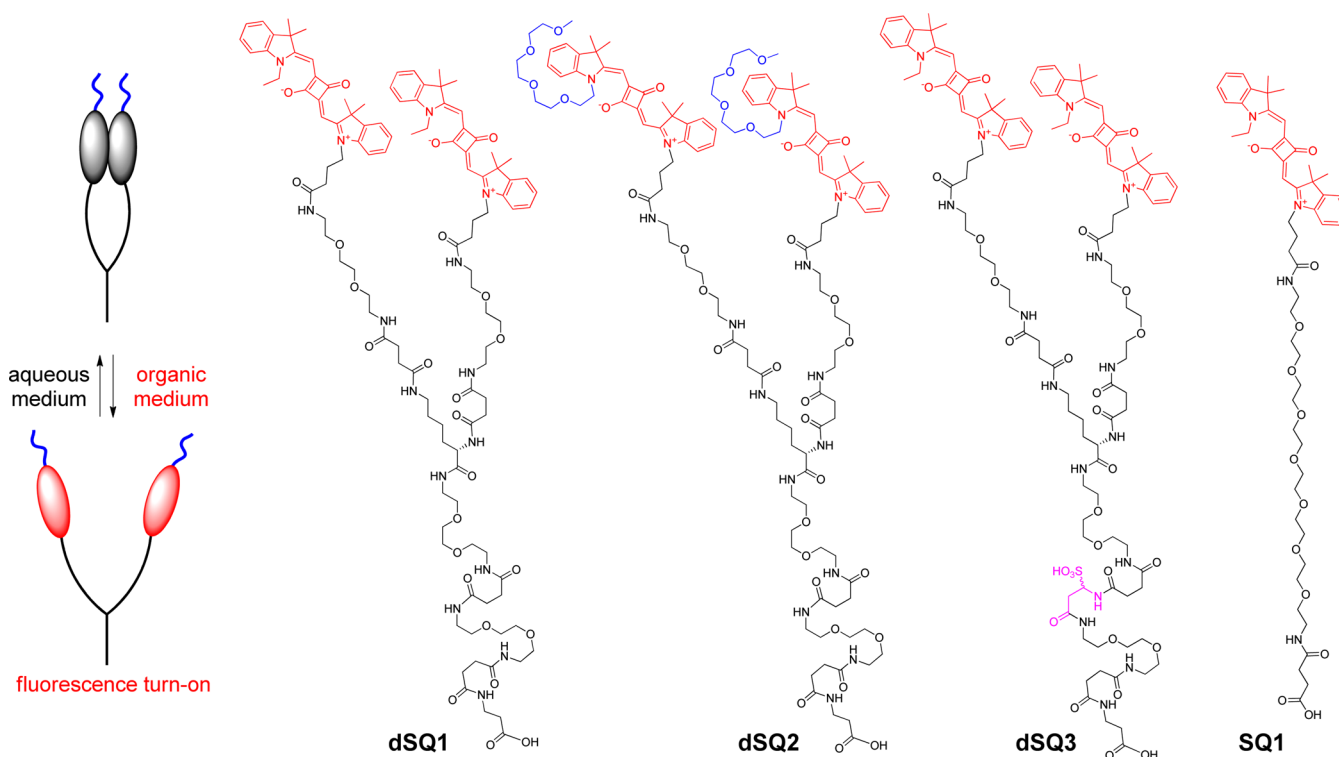


Figure 1. Principle of the functioning of squaraine dimers and their structures.

weaker sensitivity to polarity compared to blue dyes (e.g., naphthalene¹² or fluorene¹³ derivatives). Therefore, currently an intensive research is focusing on the design of polarity-sensitive fluorogenic molecules of high brightness together with red-shifted emission.^{1a,6a,10,14}

An alternative poorly explored mechanism for sensing environment polarity is the formation/disruption of H-aggregates in dye dimers. Indeed, H-aggregates obtained by π -stacking of fluorophores (Figure 1) are poorly emissive according to the exciton theory.¹⁵ These dye dimers are expected to adopt a folded form with π -stacked self-quenched dyes in aqueous media, but to unfold in the nonaqueous (less polar) environment of an organic solvent or a biomolecule, which is expected to turn on their fluorescence. These structures can be considered as foldamers¹⁶ stabilized by solvent-dependent π -stacking interactions of adjacent dyes. A similar principle was originally proposed in the 90 s for pyrene multimers, where the solvent or metal ions could disrupt the excimers, thus altering the fluorescence signal.¹⁷ However, the reported molecule was excitable only in the UV region. In the case of red and far-red cyanine dyes, homodimers were developed for the detection of nucleic acids without exploring their environment sensitivity.¹⁸ Cyanine dimers were recently applied to detect DNA hybridization,¹⁹ which is a rare example of fluorogenic dimers for sensing biomolecular interactions.

We focused our interest in squaraine dyes, because they are brighter than cyanines, owing to exceptionally high extinction coefficients ($\sim 330,000 \text{ M}^{-1} \text{ cm}^{-1}$), and their biological applications have been recently shown.²⁰ Moreover, they are noncharged and hydrophobic, which allows better control of folding due to π -stacking in aqueous media and excludes nonspecific electrostatic interactions. Formation of poorly fluorescent H-aggregates has already been shown for squaraines.²¹ Moreover, squaraine dimers with flexible chain display the capacity to fold into H-aggregates,²² a property

which was employed for detecting ions that modulate the conformational state of the dimers.²³ However, the environment sensitivity of these dimers was not explored, and they have never been designed for sensing biomolecular interactions. Moreover, these squaraine dimers were designed from aniline-based squaraines,²³ which presented limited stability due to reactions with nucleophiles in biological media.^{20e,g} On the other hand, for indolenine-based squaraines, which were not reported to be chemically unstable,²⁴ this type of dimers was not described.

Interesting biomolecules for fluorescence sensing are membrane receptors,²⁵ because they are molecular targets for drug design and delivery as well as for diagnostics of diseases. For instance, G protein-coupled receptors (GPCRs), the largest and most diverse group of membrane receptors in eukaryotes,²⁶ constitute the target for more than 30% of drugs on the market. In the present work, we selected the oxytocin receptor (OTR), which plays a crucial role in reproduction and social interaction.²⁷ Recently, we developed fluorescent ligands, utilizing the polarity-sensitive fluorogenic dye Nile Red, capable to turn on its fluorescence in response to OTR binding.^{9a} These ligands enabled the detection and quantification of OTR directly in cell suspensions as well as the background-free imaging, although they were limited by the Nile Red fluorophore, exhibiting limited brightness and photostability.

In the present work, we describe polarity-sensitive foldamers of dimeric squaraines. In aqueous media, these dimers are folded into poorly fluorescent H-aggregates, whereas their fluorescence drastically increases in organic solvents due to the unfolding. The obtained dimers are the brightest fluorogenic molecules reported to date. The tailor-made design of the dimers allowed minimizing the effects of nonspecific interactions with their biological surrounding. The fluorogenic dimers were applied for the specific detection of ligand–

Scheme 1. Synthesis of the Squaraine Dimers dSQ1, dSQ2, and dSQ3

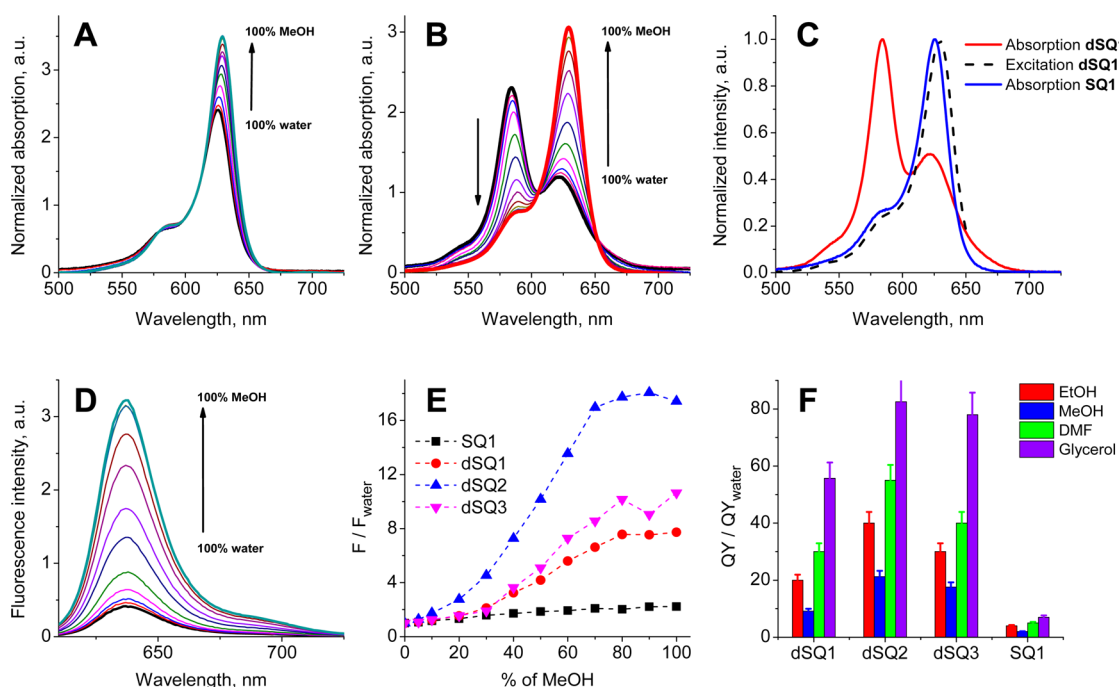
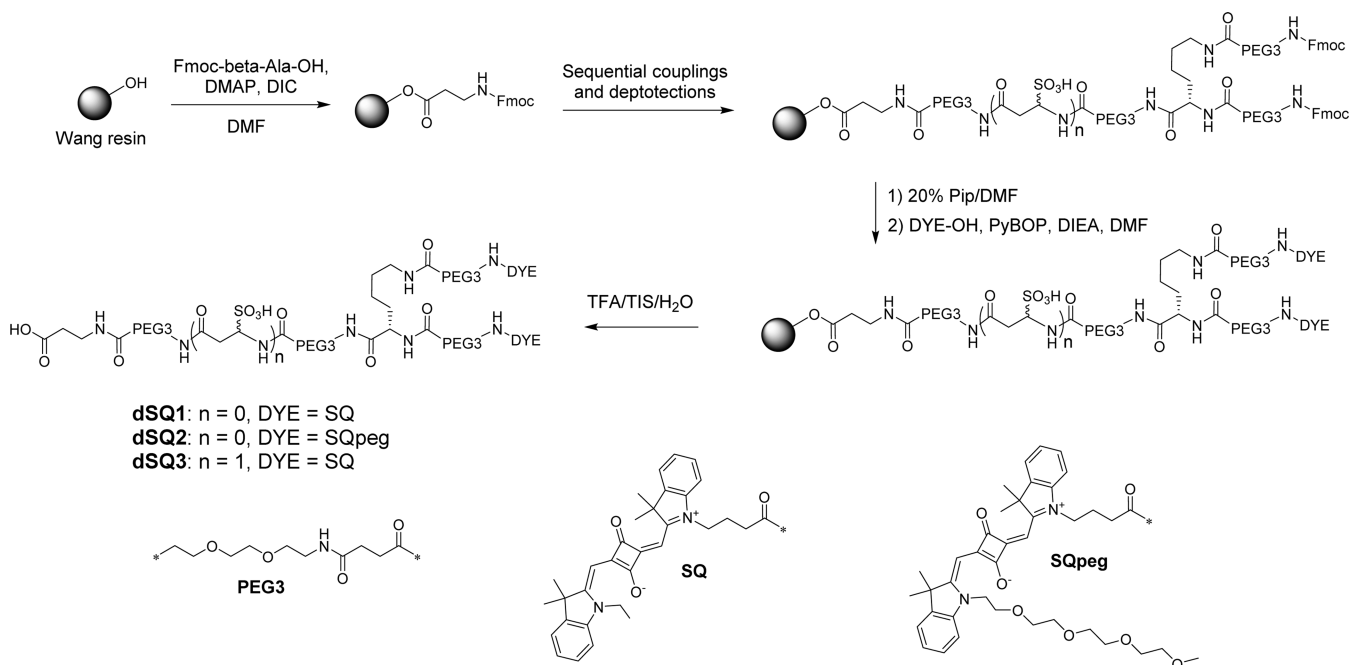


Figure 2. Absorption and fluorescence properties of the squaraine dimers and the monomer SQ1. Absorption spectra of SQ1 (A) and dSQ1 (B) in H₂O-MeOH mixtures (normalized by the absorption at 605 nm); the contents of MeOH (%) are 0, 5, 10, 20, 30, 40, 50, 60, 70, 80, 90, 100. Absorption (red) and excitation ($\lambda_{\text{emission}} = 660$ nm, black dash) spectra of dSQ1 and absorption spectra (blue) of SQ1 in water (C). Fluorescence spectra of dSQ1 (D) in H₂O-MeOH mixtures ($\lambda_{\text{excitation}} = 600$ nm); the contents of MeOH (%) are 0, 5, 10, 20, 30, 40, 50, 60, 70, 80, 90, 100. Ratio of the fluorescence intensities (F/F_{water}) of dyes in H₂O-MeOH mixtures with respect to their intensity in water (E). Turn-on properties of dSQ1, dSQ2, dSQ3, and SQ1 in organic solvents (F; ratio of quantum yield in organic solvents to that in water QY/QY_{water}).

receptor interactions, which enabled receptor imaging *in situ* on living cells with unprecedented low signal-to-background ratio.

RESULTS AND DISCUSSION

Design and Synthesis. The design of the dimers is based on the three-functional amino acid L-lysine, which allows the grafting of two dyes at the amino groups and an orthogonal

function for bioconjugation at the carboxyl group. The squaraine dyes were attached through PEG(3) chains, which are long enough to provide the dyes with some flexibility and avoid fluorescence collisional self-quenching, but short enough to keep the dyes sufficiently close to ensure their folding into π -stacked aggregates (Figure 1, dSQ1 and dSQ2). A longer PEG-based chain grafted to the carboxyl group of lysine served as a

Table 1. Fluorescence Properties of SQ1, dSQ1, dSQ2, and dSQ3^a

| solvent | ϵ | QY (SQ1), % | QY (dSQ1), % | QY (dSQ2), % | QY (dSQ3), % | τ (SQ1), ns | τ (dSQ1), ns | α_0 |
|------------------|------------|-------------|--------------|--------------|--------------|------------------|-------------------|------------|
| ethanol | 25 | 20 | 14 | 16 | 15 | 0.65 | 0.59 | 0.23 |
| DMF | 38 | 25 | 21 | 22 | 20 | ND | ND | ND |
| glycerol | 41 | 35 | 39 | 33 | 39 | 2.52 | 2.24 | 0.0 |
| phosphate buffer | 80 | 4.4 | 0.7 | 0.4 | 0.6 | ND | ND | ND |
| PBS | 80 | 4.3 | 0.7 | 0.4 | 0.6 | ND | ND | ND |
| methanol | 33 | 10 | 6.4 | 8.5 | 8.8 | 0.31 | 0.29 | 0.32 |
| water/MeOH 4/6 | ND | 8.2 | 4.7 | 6.3 | 4.4 | 0.31 | 0.30 | 0.41 |
| water/MeOH 7/3 | ND | 6.5 | 1.5 | 1.9 | 1.4 | 0.32 | 0.37 | 0.80 |
| water | 80 | 5.0 | 0.7 | 0.4 | 0.5 | ND | ND | ND |

^a ϵ is dielectric constants of solvents; QY is fluorescence quantum yield; τ is mean emission decay time; α_0 is amplitude of dark species of dSQ1 assuming 100% emissive species for SQ1; ND is not determined value.

spacer for further bioconjugation and was also expected to enhance the water solubility of the dimers. An alternative highly soluble branched linker (dSQ3) was envisaged by introduction of an α -sulfo- β -alanine moiety²⁸ in the middle of the PEG chain. Finally, a squaraine monomer SQ1 was designed for comparison (for the synthesis see SI). Due to their hydrophobicity, the squaraine moieties in the dimers dSQ1 and dSQ3 could have a tendency to interact nonspecifically with apolar sites of proteins and lipid membranes. Therefore, dSQ2 was designed, in which the ethyl group at the squaraine core was replaced with a PEG(4) residue (Figure 1). This group should change the topology of the squaraine dye from an amphiphile (polar group–apolar dye core) to a bolaamphiphile²⁹ (polar group–apolar dye core–polar group), which is expected to minimize nonspecific interactions of the dye moieties in biological media.

The synthesis of the squaraine dimers was performed on solid phase starting from the commercially available Wang (*p*-alkoxybenzyl alcohol)-PS resin (Scheme 1). First, β -alanine residue was introduced by activation of the resin with DIC in the presence of 4-DMAP in DMF. Then, its deprotected amino group was coupled to the ester species of Fmoc-NH-PEG3-COOH³⁰ following a PyBOP *in situ* activation. α -Sulfo- β -alanine amino acid was then incorporated in the case of the synthesis of dSQ3 according to a described protocol.²⁸ The resulting chains were elongated with Fmoc-NH-PEG3-COOH, Fmoc-L-Lys(Fmoc)-OH and again with Fmoc-NH-PEG3-COOH. The introduction of fluorophores SQ-OH and SQpeg-OH (for the synthesis see SI) was performed on solid phase by activation with PyBOP in the presence of DIEA in DMF. After completion of couplings, the chains were cleaved from the solid phase in concentrated TFA and purified by semipreparative HPLC. The identity and purity of the squaraine dimers dSQ1, dSQ2 and dSQ3 were confirmed by LC-HRMS.

Fluorogenic Properties in Solvents. The spectroscopic properties of the squaraine dimers dSQ1, dSQ2, and dSQ3 and the monomer SQ1 were studied in solvents of different polarities (Figure 2, Table 1; Figure S1 and Table S1 in SI). Of particular interest were the absorption spectra of the squaraine dimers in water. In contrast to the typical absorption spectrum of SQ1 with a maximum at 626 nm and a small short-wavelength shoulder (Figure 2A,C), all three dimers exhibited a major band maximum at 584–587 nm with a minor shoulder at longer wavelength (Figure 2B,C; Figure S2 in SI). When water solution of dSQ1 was titrated with methanol, this short-wavelength band decreased in favor of the long-wavelength band at 629 nm, which became dominant already at 40% of

MeOH in water (Figure 2B; Figure S3 in SI). In sharp contrast, SQ1 displayed relatively minor changes in the absorption spectra (Figure 2A). In neat methanol and other organic solvents all three dimers showed nearly the same absorption maxima without additional short-wavelength maximum (Figure S1 in SI). In fluorescence spectra, an increase of the methanol concentration in water from 0 to 100% resulted in an \sim 8-fold intensity increase for the dimer dSQ1 and only \sim 2-fold for the monomer SQ1 (Figure 2E). dSQ2 was found to show the most efficient 18-fold fluorescence jump between water and methanol.

In order to further identify the species in water absorbing at 584 nm, fluorescence excitation spectra were recorded (Figure 2C). The excitation spectrum of dSQ1 in water differed from its absorption spectrum and was nearly identical to the absorption spectrum of SQ1 (Figure 2C). This clearly shows that the species absorbing at 584 nm are practically non-fluorescent and that the fluorescence of SQ1 likely originates from a small fraction of unfolded squaraine dimers. The same feature was observed with dSQ2 and dSQ3 (Figure S2 in SI). Based on previous reports on squaraines,^{21c} the short-wavelength absorption band can be assigned to H-aggregates formed as a consequence of the folding of the squaraine dimer (Figure 1). This folding can be stabilized by hydrophobic and π -stacking interactions of the squaraine units in water. On the other hand, in methanol the H-aggregates were disrupted, resulting in absorption spectra that corresponded to the spectrum of the monomer SQ1.

To check the intramolecular nature of the H-aggregates, we studied the absorption spectra of the squaraine dimers at different concentrations (Figure S4 in SI). The ratio between the two absorption bands at 584 and 626 nm remained constant over a large concentration range, indicating that the short-wavelength species were of intramolecular nature. While the core-PEGylated squaraine derivative dSQ2 and the squaraine derivative with an α -sulfo- β -alanine moiety dSQ3 displayed identical absorption spectra in the concentration range from 20 nM to 2 μ M, a third red-shifted band appeared in the absorption spectra of dSQ1 starting from 1 μ M concentration. This band can be assigned to intermolecular aggregates which formed due to the lower water solubility of dSQ1 compared to the other dimers.

We were pleased to find that the fluorescence quantum yields of the squaraine dimers in water were \sim 10 times lower than that of the monomer, whereas in organic solvents the differences were much less pronounced (Table 1). Thus, the folding of dSQ1–3 into H-aggregates ensured their low quantum yields in water. Remarkably, the presence of inorganic

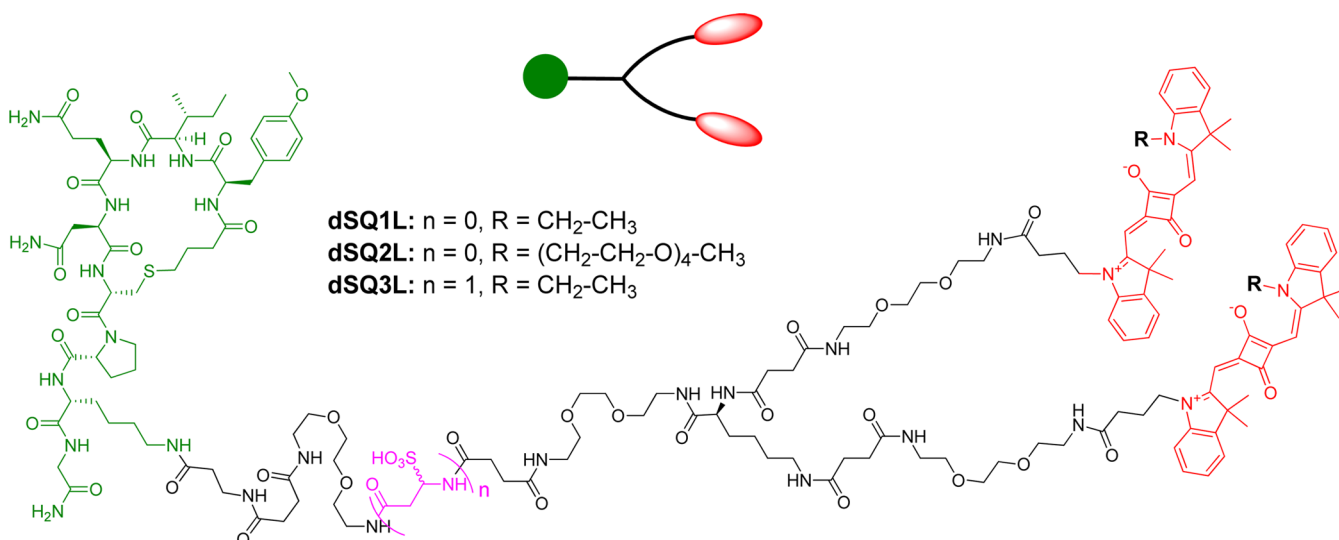


Figure 3. Structures of squaraine dimers conjugated to Lys⁸-CBT.

salts in water (phosphate buffer and phosphate buffer saline) did not affect the quantum yield values. Taking into account that the H-aggregates are nonfluorescent, the observed values of quantum yield 0.4–0.7% in aqueous media likely originate from unfolded dimers. The fraction of unfolded dimers was the lowest in water and the highest in organic solvents, where the folded structure with H-aggregated dimer was not favored due to solvation of the squaraine units. Overall, the comparison of the quantum yield values in organic solvents with those in water (Table 1) showed that **dsSQ1–3** dimers are 5–10 times more sensitive to polarity changes than the monomer. However, the response to polarity is nonlinear, focusing in the range of highly polar solvents between water and methanol (Figure 2E), where the modulation of the intramolecular H-aggregation takes place. This polarity range is particularly relevant to biomolecule–water interfaces, important for biosensing. Finally, in viscous media such as glycerol, the dimers exhibited an increase in the quantum yield by 4–5-fold compared to methanol, which was similar to that of the monomer (3.5-fold increase).

To further characterize the fluorescence enhancement in organic solvents, we performed time-resolved fluorescence measurements for **dsSQ1** and **SQ1** in different solvents (see Table S2 in SI). For all solvents, including water–methanol mixtures, the mean lifetimes of **dsSQ1** were close to those of **SQ1**, whereas these two molecules displayed strong differences in the quantum yields. This observation clearly indicates the presence of dark (nonfluorescent) species (with lifetimes shorter than the 20 ps resolution of our setup) in the dimer **dsSQ1**, which decreased the overall quantum yield without contributing to the mean lifetime. These dark species can be clearly assigned to H-aggregates identified from the absorption spectra (Figure 2B). The small fraction of emissive species showing the same lifetime as **SQ1** corresponds probably to unfolded dimers, in line with the excitation spectra (Figure 2C). The calculated content of dark species increased rapidly on increase in the water content in the mixtures with methanol (Table 1), corroborating the observed growth of the short-wavelength band of the H-aggregate (Figure 2B). The mean lifetime in viscous solvent glycerol was larger than in other solvents in line with the difference in their quantum yields. Therefore, the viscosity affects the intrinsic properties of the

squaraine core by decreasing the nonradiative decay rates, which is typically observed for molecular rotors.^{3b}

Overall, we achieved a fluorogenic response to the environment using dimers of squaraines that present remarkably high extinction coefficient ($\epsilon \sim 2 \times 330,000 \text{ M}^{-1} \text{ cm}^{-1}$) and relatively good quantum yield in the turn-on state (QY up to 40%). To the best of our knowledge, the brightness (expressed as $\epsilon \times \text{QY}$) of this construct in the on-state is far better than any existing fluorogenic molecule reported to date. For comparison, Nile Red, one of the brightest fluorogenic dyes based on charge-transfer mechanism (solvatochromism) is about 10-fold less bright ($\epsilon = 43,000 \text{ M}^{-1} \text{ cm}^{-1}$ and QY $\geq 50\%$ in organic media).^{11b,31} However, we admit that the direct comparison with the charge-transfer dyes should be done with care, because solvatochromic dyes operate by a different mechanism and present important property of linear correlation with the solvent polarity,^{2a} unlike our dimeric constructs showing nonlinear responses in a narrow polarity range between aqueous and organic media. Finally, these dimeric constructs work in the far-red region (630–700 nm), which is still compatible with the classical microscopy setups for cellular imaging and, at the same time, already fits to the optical window of live tissues for *in vivo* imaging.³²

Application of the Dimers for the Detection of the Oxytocin Receptor. To explore the potency of the squaraine dimers in cellular studies, we coupled **dsSQ1**, **dsSQ2**, and **dsSQ3** to a modified carbetocin (CBT) Lys⁸-CBT,^{9a} an oxytocin receptor ligand, in order to obtain conjugates **dsSQ1L**, **dsSQ2L**, and **dsSQ3L** (Figure 3 and Scheme S7 in SI). The spectroscopic properties of the obtained conjugates were similar to those of the parent squaraine dimers (Table S1 in SI).

In order to check the possible nonspecific interactions of the dimeric OTR probes with serum proteins and lipid membranes, we titrated their aqueous solutions with bovine serum albumin (BSA) and lipid vesicles (Figure 4). BSA, the key component of serum, and lipid vesicles, the models of biological membranes, can bind a variety of lipophilic molecules and thus provide false positive responses with environment-sensitive probes.^{9a} Here, we observed that **dsSQ1L** and **dsSQ3L** increased their fluorescence intensity on addition of BSA and large unilamellar vesicles (composed of dioleoylphosphatidylcholine, DOPC), suggesting that they can bind nonspecifically and lose their

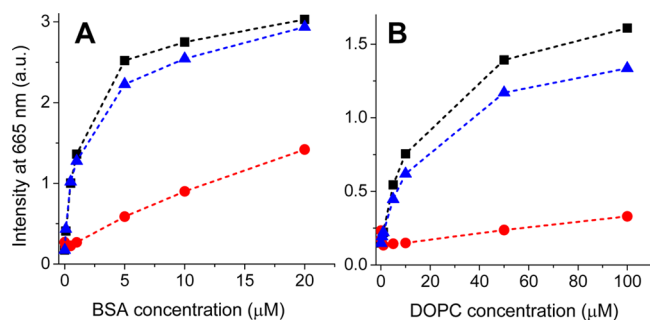


Figure 4. Studies of nonspecific interactions of the squaraine dimers with BSA and lipid vesicles (composed of DOPC). Fluorescence intensities of **dsQ1L** (black squares), **dsQ2L** (red circles), and **dsQ3L** (blue triangles) in phosphate buffer as a function of BSA (A) or DOPC (B) concentrations.

intramolecular H-aggregation. Surprisingly, the negatively charged sulfonate group in **dsQ3L** did not decrease the nonspecific binding in comparison to **dsQ1L**. In contrast, **dsQ2L**, the compound with the core-pegylated squaraine, displayed relatively low nonspecific binding, as the intensity changes were small. This indicates that the PEG groups from both ends of the squaraine dye (bolaamphiphile topology) in **dsQ2L** prevent the dye from interaction with lipids or BSA, thus preserving its intramolecular H-aggregation.

Confocal microscopy studies with the squaraine dimers were performed on adherent HEK293 cells expressing the oxytocin receptor fused to the green fluorescent protein (GFP-OTR cells) (Figure 5A–C). After addition of 10 nM of the dimers to the cells, we observed a strong fluorescence in the “squaraine” channel (excitation at 635 nm) at the cell plasma membranes, which co-localized with the fluorescence in the “GFP” channel (excitation at 488 nm). Moreover, the different GFP intensities for different cells, related to varied OTR expression, correlated well with the fluorescence intensity of the squaraine dimers

(Figure S5 in SI), indicating that ligand signal is proportional to the receptor expression level. To verify the specificity of the new fluorescent ligands to OTR, we performed competition assays with a large excess of unlabeled CBT ligand (Figure 5A–C). These experiments showed that all three dimers could bind specifically to OTR, but **dsQ2L** displayed much lower nonspecific fluorescence than **dsQ1L** and **dsQ3L** from cell membranes, in line with our data on lipid vesicles (Figure 4). To confirm our conclusions, a quantitative analysis of the obtained images was performed. The average fluorescence intensities from cell membranes in the “squaraine” channel corrected for varied receptor expression (through division by the intensity in the “GFP” channel) were compared for all three probes without and with CBT competitor (Figure 5D). The obtained intensity values without CBT decreased in the order **dsQ1L** > **dsQ3L** > **dsQ2L**, whereas with CBT, which reflects the nonspecific interactions, it was **dsQ3L** ~ **dsQ1L** >> **dsQ2L**. By calculating the ratio between the total (OTR cells) and the nonspecific (OTR cells + CBT) fluorescence, we confirmed that squaraine dimer **dsQ2L**, despite its less bright character, was the most specific for detecting the oxytocin receptor at the surface of living cells (Figure 5E). Another important feature was the exceptionally low background observed for all three ligands, so that the signal-to-background ratio was 100–250 (Figure 5F), which is clearly related to the fluorogenic nature of the ligands.

To further characterize the local environment of the ligands bound to OTR, we performed fluorescence lifetime imaging (FLIM) on adherent HEK293 cells expressing the wild-type oxytocin receptor (wt-OTR cells). The mean lifetime for the three CBT-derived probes at the level of cell membranes was around 2.5 ns (Figure 6). Remarkably, this value was close to those obtained for the squaraine dimers in glycerol (Table 1), suggesting that after binding to the receptor, the squaraine units experienced viscous and poorly hydrated environment. Together with the observed excellent brightness and signal-

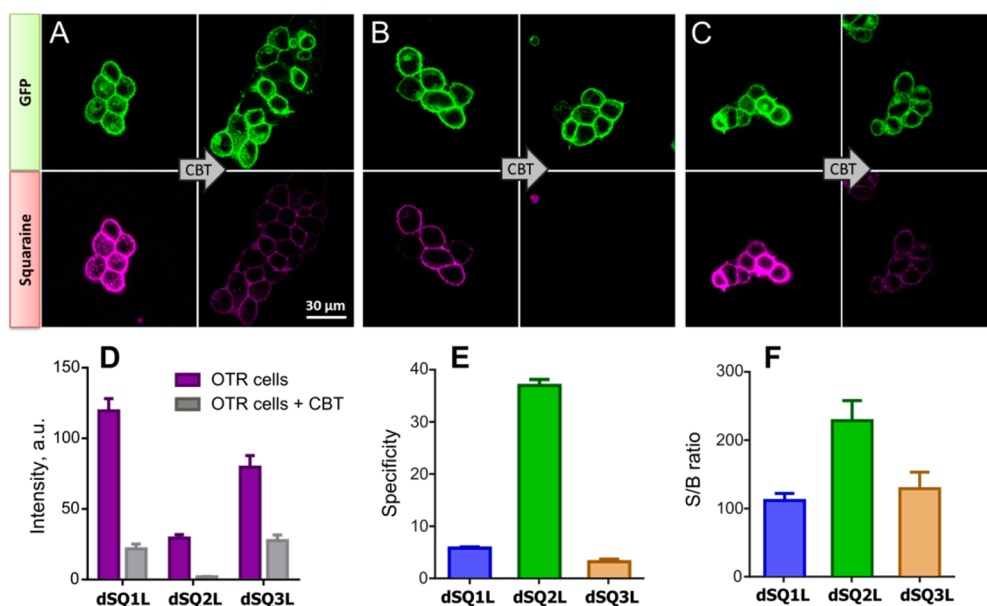


Figure 5. Confocal microscopy studies. Confocal images of GFP-OTR cells with 10 nM of **dsQ1L** (A), **dsQ2L** (B), or **dsQ3L** (C) with or without nonlabeled CBT (2 μM). Average fluorescence intensities from the cell surface before and after the addition of CBT (D). Specificity of the probes: ratio between specific and nonspecific (with CBT) membrane fluorescence (E). Signal-to-background ratio (F). Bars represent means, and error bars show SEM values (obtained from four images).

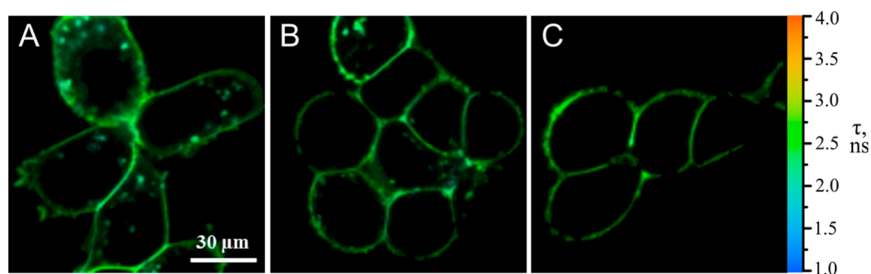


Figure 6. Fluorescence lifetime imaging of dSQ1L (A), dSQ2L (B), and dSQ3L (C) at the surface of the adherent HEK293 cells expressing wt-OTR.

to-background ratios, FLIM data suggest that the dimers respond to receptor binding by unfolding of their intermolecular H-aggregates, as it was observed in organic solvents.

Finally, to further stress the fluorogenic character of the best squaraine dimer probe dSQ2L, we performed a comparative confocal imaging with the previously developed^{9a} nonfluorogenic lissamine rhodamine B OTR probe LRh-CBT (Figure 7)

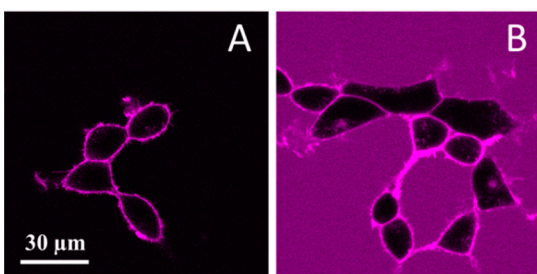


Figure 7. Turn-on properties of squaraine dimers. Confocal images of HEK293 cells expressing OTR with 100 nM of dSQ2L (A) and LRh-CBT (B).

at 100 nM. The signal of dSQ2L at the cell membranes was 40-fold higher than in the extracellular medium, whereas for LRh-CBT, the signal-to-background ratio was only ~ 2 . Thus, in aqueous solution our dimer ligand being in the folded self-quenched state does not contribute to the background signal, in contrast to LRh-CBT. After binding to the membrane receptor, the environment of our probes should contain much less water, which leads to the unfolding of the dimer that turns on the fluorescence of the ligand. This change in the environment of the labeled ligand on binding to OTR is in line with our previous study with the Nile Red-CBT conjugate, which showed a strong decrease in the polarity of the Nile Red environment on binding to OTR.^{9a}

CONCLUSIONS

In the present work, we describe a concept of fluorogenic dimers of dyes, which are self-quenched in aqueous media due to H-aggregation, but capable to unfold in organic media so that their fluorescence is turned on. To validate this concept, we designed and synthesized three dimers of two different squaraine dyes which are linked together to a lysine core through PEG(3) spacers. In aqueous media, these dimers showed the characteristic absorption band of intramolecular H-aggregates that were nonfluorescent. In organic solvents, the unfolding of the dimer disrupted the H-aggregate, turning its fluorescence on. All three fluorogenic dimers were grafted to a ligand of the oxytocin receptor (carbetocin) and tested in cells. Among the three probes, the one derived from the core-

PEGylated squaraine was found to be the most potent in sensing OTR at the cell surface with high sensitivity and low nonspecific binding to the cell membrane and serum proteins. The obtained constructs are the brightest polarity-sensitive fluorogenic molecules reported to date, owing to their high extinction coefficient ($\sim 660,000 \text{ M}^{-1} \text{ cm}^{-1}$) and quantum yield (up to 40%) in the on-state. They are also among the first polarity-sensitive fluorogenic dyes operating in the far-red region. We anticipate that the concept of polarity-sensitive fluorogenic dimers could be extended to other dyes, such as cyanines, rhodamines, etc., because the formation of self-quenched H-aggregates is a general property of flat aromatic fluorophores. Therefore, this concept will pave the way to new generation of bright fluorogenic probes of different colors for target-specific ultrasensitive detection of proteins (particularly membrane receptors) in living cells.

ASSOCIATED CONTENT

Supporting Information

Materials and material section. This material is available free of charge via the Internet at <http://pubs.acs.org>.

AUTHOR INFORMATION

Corresponding Authors

dominique.bonnet@unistra.fr
andrey.klymchenko@unistra.fr

Notes

The authors declare no competing financial interest.

ACKNOWLEDGMENTS

This work was supported by ANR JCJC (ANR-11-JS07-014-01), CNRS, INSERM, and the University of Strasbourg. We warmly thank Pascale Buisine, Dr. Justine Viéville, and Patrick Wehrung from the Service de Chimie Analytique (SCA) for LC-MS and RMN analyses. I.A.K. was supported by a fellowship from the Ministère de l'Éducation Nationale, de l'Enseignement Supérieur et de la Recherche.

REFERENCES

- (a) Li, X.; Gao, X.; Shi, W.; Ma, H. *Chem. Rev.* **2014**, *114*, 590. (b) Grimm, J. B.; Heckman, L. M.; Lavis, L. D. *Prog. Mol. Biol. Transl. Sci.* **2013**, *113*, 1. (c) Nadler, A.; Schultz, C. *Angew. Chem., Int. Ed.* **2013**, *52*, 2408. (d) Santos-Figueroa, L. E.; Moragues, M. E.; Climent, E.; Agostini, A.; Martínez-Máñez, R.; Sancenón, F. *Chem. Soc. Rev.* **2013**, *42*, 3489. (e) Devaraj, N. K.; Hilderbrand, S.; Upadhyay, R.; Mazitschek, R.; Weissleder, R. *Angew. Chem., Int. Ed.* **2010**, *49*, 2869.
- (a) Reichardt, C. *Chem. Rev.* **1994**, *94*, 2319. (b) Grabowski, Z. R.; Rotkiewicz, K.; Rettig, W. *Chem. Rev.* **2003**, *103*, 3899.
- (a) Haidekker, M. A.; Theodorakis, E. A. *Org. Biomol. Chem.* **2007**, *5*, 1669. (b) Kuimova, M. K.; Yahioglu, G.; Levitt, J. A.; Suhling, K. *J. Am. Chem. Soc.* **2008**, *130*, 6672.

- (4) (a) Demchenko, A. P.; Tang, K. C.; Chou, P. T. *Chem. Soc. Rev.* **2013**, *42*, 1379. (b) Klymchenko, A. S.; Demchenko, A. P. *Phys. Chem. Chem. Phys.* **2003**, *5*, 461.
- (5) (a) Loving, G. S.; Sainlos, M.; Imperiali, B. *Trends Biotechnol.* **2010**, *28*, 73. (b) Klymchenko, A. S.; Mely, Y. *Prog. Mol. Biol. Transl. Sci.* **2013**, *113*, 35. (c) Demchenko, A. P.; Mély, Y.; Dupontail, G.; Klymchenko, A. S. *Biophys. J.* **2009**, *96*, 3461. (d) Yang, Z.; Cao, J.; He, Y.; Yang, J. H.; Kim, T.; Peng, X.; Kim, J. S. *Chem. Soc. Rev.* **2014**, *43*, 4563.
- (6) (a) Loving, G.; Imperiali, B. *J. Am. Chem. Soc.* **2008**, *130*, 13630. (b) Vázquez, M. E.; Blanco, J. B.; Imperiali, B. *J. Am. Chem. Soc.* **2005**, *127*, 1300.
- (7) (a) Shvadchak, V. V.; Klymchenko, A. S.; De Rocquigny, H.; Mély, Y. *Nucleic Acids Res.* **2009**, *37*, e25. (b) Strizhak, A. V.; Postupalenko, V. Y.; Shvadchak, V. V.; Morellet, N.; Guittet, E.; Pivovarenko, V. G.; Klymchenko, A. S.; Mély, Y. *Bioconjugate Chem.* **2012**, *23*, 2434.
- (8) (a) Postupalenko, V. Y.; Shvadchak, V. V.; Dupontail, G.; Pivovarenko, V. G.; Klymchenko, A. S.; Mély, Y. *Biochim. Biophys. Acta* **2011**, *1808*, 424. (b) Zamotaiev, O. M.; Postupalenko, V. Y.; Shvadchak, V. V.; Pivovarenko, V. G.; Klymchenko, A. S.; Mély, Y. *Org. Biomol. Chem.* **2014**, *12*, 7036.
- (9) (a) Karpenko, I. A.; Kreder, R.; Valencia, C.; Villa, P.; Mendre, C.; Mouillac, B.; Mély, Y.; Hibert, M.; Bonnet, D.; Klymchenko, A. S. *ChemBioChem* **2014**, *15*, 359. (b) Prifti, E.; Reymond, L.; Umebayashi, M.; Hovius, R.; Riezman, H.; Johnsson, K. *ACS Chem. Biol.* **2014**, *9*, 606.
- (10) Touthkine, A.; Kraynov, V.; Hahn, K. *J. Am. Chem. Soc.* **2003**, *125*, 4132.
- (11) (a) Greenspan, P.; Fowler, S. D. *J. Lipid Res.* **1985**, *26*, 781. (b) Kucherak, O. A.; Oncul, S.; Darwich, Z.; Yushchenko, D. A.; Arntz, Y.; Didier, P.; Mely, Y.; Klymchenko, A. S. *J. Am. Chem. Soc.* **2010**, *132*, 4907.
- (12) (a) Weber, G.; Farris, F. J. *Biochemistry* **1979**, *18*, 3075. (b) Slavik, J. *Biochim. Biophys. Acta* **1982**, *694*, 1.
- (13) Kucherak, O. A.; Didier, P.; Mély, Y.; Klymchenko, A. S. *J. Phys. Chem. Lett.* **2010**, *1*, 616.
- (14) (a) Giordano, L.; Shvadchak, V. V.; Fauerbach, J. A.; Jares-Erijman, E. A.; Jovin, T. M. *J. Phys. Chem. Lett.* **2012**, *3*, 1011. (b) Kucherak, O. A.; Richert, L.; Mély, Y.; Klymchenko, A. S. *Phys. Chem. Chem. Phys.* **2012**, *14*, 2292. (c) Niko, Y.; Kawauchi, S.; Konishi, G. I. *Chem.—Eur. J.* **2013**, *19*, 9760. (d) Lu, Z.; Lord, S. J.; Wang, H.; Moerner, W. E.; Twieg, R. J. *J. Org. Chem.* **2006**, *71*, 9651. (e) Niko, Y.; Cho, Y.; Kawauchi, S.; Konishi, G. I. *RSC Adv.* **2014**, *4*, 36480. (f) Lord, S. J.; Lu, Z.; Wang, H.; Willets, K. A.; Schuck, P. J.; Lee, H. L. D.; Nishimura, S. Y.; Twieg, R. J.; Moerner, W. E. *J. Phys. Chem. A* **2007**, *111*, 8934.
- (15) Kasha, M.; Rawls, H. R.; El-Bayoumi, M. A. *Pure Appl. Chem.* **1965**, *11*, 371.
- (16) (a) Hecht, S.; Huc, I. *Foldamers: Structure, Properties, and Applications*; Wiley-VCH: Weinheim, 2007. (b) Hill, D. J.; Mio, M. J.; Prince, R. B.; Hughes, T. S.; Moore, J. S. *Chem. Rev.* **2001**, *101*, 3893.
- (17) (a) Aoki, I.; Kawabata, H.; Nakashima, K.; Shinkai, S. *Chem. Commun.* **1991**, 1771. (b) Nishizawa, S.; Kato, Y.; Teramae, N. *J. Am. Chem. Soc.* **1999**, *121*, 9463.
- (18) Rye, H. S.; Yue, S.; Wemmer, D. E.; Quesada, M. A.; Haugland, R. P.; Mathies, R. A.; Glazer, A. N. *Nucleic Acids Res.* **1992**, *20*, 2803.
- (19) (a) Ikeda, S.; Kubota, T.; Yuki, M.; Okamoto, A. *Angew. Chem., Int. Ed.* **2009**, *48*, 6480. (b) Okamoto, A. *Chem. Soc. Rev.* **2011**, *40*, 5815.
- (20) (a) Ajayaghosh, A. *Acc. Chem. Res.* **2005**, *38*, 449. (b) Sreejith, S.; Carol, P.; Chithra, P.; Ajayaghosh, A. *J. Mater. Chem.* **2008**, *18*, 264. (c) Markova, L. I.; Terpetschnig, E. A.; Patsenker, L. D. *Dyes Pigm.* **2013**, *99*, 561. (d) Oswald, B.; Patsenker, L.; Duschl, J.; Szmajcinski, H.; Wolfbeis, O. S.; Terpetschnig, E. *Bioconjugate Chem.* **1999**, *10*, 925. (e) Sreejith, S.; Divya, K. P.; Ajayaghosh, A. *Angew. Chem., Int. Ed.* **2008**, *47*, 7883. (f) Anees, P.; Sreejith, S.; Ajayaghosh, A. *J. Am. Chem. Soc.* **2014**, *136*, 13233. (g) Ros-Lis, J. V.; García, B.; Jiménez, D.; Martínez-Mañez, R.; Sancenón, F.; Soto, J.; Gonzalvo, F.; Valdecabres, M. C. *J. Am. Chem. Soc.* **2004**, *126*, 4064.
- (21) (a) Chen, H.; Farahat, M. S.; Law, K. Y.; Whitten, D. G. *J. Am. Chem. Soc.* **1996**, *118*, 2584. (b) Chen, H.; Herkstroeter, W. G.; Perlstein, J.; Law, K. Y.; Whitten, D. G. *J. Phys. Chem.* **1994**, *98*, 5138. (c) Das, S.; Thomas, K. G.; Thomas, K. J.; Madhavan, V.; Liu, D.; Kamat, P. V.; George, M. V. *J. Phys. Chem.* **1996**, *100*, 17310.
- (22) Liang, K.; Farahat, M. S.; Perlstein, J.; Law, K. Y.; Whitten, D. G. *J. Am. Chem. Soc.* **1997**, *119*, 830.
- (23) (a) Arunkumar, E.; Chithra, P.; Ajayaghosh, A. *J. Am. Chem. Soc.* **2004**, *126*, 6590. (b) Block, M. A. B.; Hecht, S. *Macromolecules* **2004**, *37*, 4761. (c) Arunkumar, E.; Ajayaghosh, A.; Daub, J. *J. Am. Chem. Soc.* **2005**, *127*, 3156.
- (24) (a) Markova, L. I.; Malinovskii, V. L.; Patsenker, L. D.; Häner, R. *Org. Biomol. Chem.* **2012**, *10*, 8944. (b) Pisoni, D. D. S.; De Abreu, M. P.; Petzhold, C. L.; Rodembusch, F. S.; Campo, L. F. *J. Photochem. Photobiol., A* **2013**, *252*, 77.
- (25) (a) Daly, C. J.; McGrath, J. C. *Pharmacol. Ther.* **2003**, *100*, 101. (b) Sridharan, R.; Zuber, J.; Connelly, S. M.; Mathew, E.; Dumont, M. E. *Biochim. Biophys. Acta* **2014**, *1838*, 15.
- (26) (a) Albizu, L.; Teppaz, G.; Seyer, R.; Bazin, H.; Ansanay, H.; Manning, M.; Mouillac, B.; Durroux, T. *J. Mater. Chem.* **2007**, *50*, 4976. (b) Rosenbaum, D. M.; Rasmussen, S. G. F.; Kobilka, B. K. *Nature* **2009**, *459*, 356.
- (27) (a) Gimpl, G.; Fahrenholz, F. *Physiol. Rev.* **2001**, *81*, 629. (b) MacDonald, K.; MacDonald, T. M. *Harv. Rev. Psychiatry* **2010**, *18*, 1.
- (28) Romieu, A.; Brossard, D.; Hamon, M.; Outaabout, H.; Portal, C.; Renard, P. Y. *Bioconjugate Chem.* **2008**, *19*, 279.
- (29) Fuhrhop, J. H.; Wang, T. *Chem. Rev.* **2004**, *104*, 2901.
- (30) Soriano, A.; Ventura, R.; Molero, A.; Hoen, R.; Casado, V.; Corte, A.; Fanelli, F.; Albericio, F.; Lluís, C.; Franco, R.; Royo, M. J. *Med. Chem.* **2009**, *52*, 5590.
- (31) Deda, M. L.; Ghedini, M.; Aiello, I.; Pugliese, T.; Barigelletti, F.; Accorsi, G. *J. Organomet. Chem.* **2005**, *690*, 857.
- (32) (a) Shcherbo, D.; Merzlyak, E. M.; Chepurnykh, T. V.; Fradkov, A. F.; Ermakova, G. V.; Solovieva, E. A.; Lukyanov, K. A.; Bogdanova, E. A.; Zarskiy, A. G.; Lukyanov, S.; Chudakov, D. M. *Nat. Methods* **2007**, *4*, 741. (b) Lin, M. Z.; McKeown, M. R.; Ng, H. L.; Aguilera, T. A.; Shaner, N. C.; Campbell, R. E.; Adams, S. R.; Gross, L. A.; Ma, W.; Alber, T.; Tsien, R. Y. *Chem. Biol.* **2009**, *16*, 1169. (c) Egawa, T.; Hanaoka, K.; Koide, Y.; Ujita, S.; Takahashi, N.; Ikegaya, Y.; Matsuki, N.; Terai, T.; Ueno, T.; Komatsu, T.; Nagano, T. *J. Am. Chem. Soc.* **2011**, *133*, 14157.